AMSR-E/Aqua Daily L3 25 km Brightness Temperature & Sea Ice Concentration Polar Grids, Version 4

USER GUIDE

How to Cite These Data

As a condition of using these data, you must include a citation:

Markus, T., J. C. Comiso, L. Boisvert, and W. N. Meier. 2025. *AMSR-E/Aqua Daily L3 25 km Brightness Temperature & Sea Ice Concentration Polar Grids, Version 4*. [Indicate subset used]. Boulder, Colorado USA. NASA National Snow and Ice Data Center Distributed Active Archive Center. https://doi.org/10.5067/QD0EB4TQGG6A. [Date Accessed].

FOR QUESTIONS ABOUT THESE DATA, CONTACT NSIDC@NSIDC.ORG

FOR CURRENT INFORMATION, VISIT https://nsidc.org/data/AE_SI25

National Snow and Ice Data Center

TABLE OF CONTENTS

1 DETAILED DATA DESCRIPTION

1.1 Parameters

This data set (AE_SI25) reports average daily, 25 km resolution, horizontally and vertically polarized brightness temperatures (T_b) at six frequencies—6.9 GHz, 10.7 GHz, 18.7 GHz, 23.8 GHz, 36.5 GHz, and 89.0 GHz. It also reports daily sea ice concentrations derived using the Enhanced NASA Team (NT2) algorithm and daily sea ice concentration differences between the NT2 and the legacy AMSR Basic Bootstrap Algorithm (ABA). Data are provided on Northern and Southern Hemisphere, polar stereographic grids.

The data are derived from observations acquired by the Advanced Microwave Scanning Radiometer for EOS (AMSR-E) on board the NASA Aqua satellite.

1.2 File Information

1.2.1 File Format

Data are provided in Hierarchical Data Format - Earth Observing System 5 (HDF-EOS5).

1.2.2 Data Fields

T_bs, sea ice concentrations, and sea ice concentration differences are written as 2-byte, signed data fields to separate North and South Pole data groups as follows:

HDFEOS/GRIDS/NpPolarGrid25km/Data Fields/
HDFEOS/GRIDS/SpPolarGrid25km/Data Fields/

The NpPolarGrid25km and SpPolarGrid25km data groups also contain latitude and longitude grids, named “lat” and “lon”, respectively, plus the NetCDF dimension scales[1] “XDim” and “YDim”.

1.2.2.1 Naming Convention

Daily average horizontally polarized (H) and vertically polarized (V) T_bs, at each frequency (F), sea ice concentrations, and sea ice concentration differences are reported for ascending orbits (ASC), descending orbits (DSC), and as a daily average (DAY).

Data fields are named according to the following convention:

[1]For more information about NetCDF dimension scales, see NetCDF-4 Dimensions and HDF5 Dimension Scales.

Example

SI_25km_NH_06H_ASC

SI_25km_NH_ICECON_ASC

SI_25km_NH_ICEDIFF_ASC

Naming Convention

SI_[RES]km_[HEM]_[PARAM]_[ORBIT]

The variables above are described in Table 1:

Table 1. Data Field Variable Names and Descriptions

Variable Name	Description
RES	25 (25 km)
HEM	NH (N. Hemisphere) or SH (S. Hemisphere)
PARAM	One of: • FPOL (frequency and polarization): E.g., 06H = 6.9 GHz, horizontal polarization; 06V = 6.9 GHz, vertical polarization • ICECON: Sea ice conc. • ICEDIFF: Sea ice conc. difference
ORBIT	One of: • ASC (ascending average) • DSC (descending average) • DAY (daily average)

1.2.2.2 Brightness Temperature (Tbs)

T_bs are scaled by a factor of 10 (i.e., have a scale factor = 0.1) when written to the data fields. To recover T_bs in kelvins, multiply the stored value by 0.1. E.g., a stored value of 2673 = 267.3 K. Missing data are denoted by a value of 0.

1.2.2.3 Sea Ice Concentration

Sea ice concentrations are reported as percentages, with values ranging from 1 to 100. A value of 110 = missing data, while 0 = open water and 120 = land.

1.2.2.4 Sea Ice Concentration Difference

Sea ice concentration differences, calculated as ICEDIFF = ABA - NT2, are provided for users who wish to recover the value of the legacy ABA algorithm (i.e., ABA = ICECON + ICEDIFF). However,

this approach is not without its quirks. For example, in pixels flagged as land (120) by both the ABA and NT2 algorithms, differencing these values produces “0,” the value ICECON uses to identify open ocean. Furthermore, because the algorithms utilize different land masks, the same pixel may be flagged as land (120) by one algorithm and open water (0) by the other. As such, ICEDIFF should be used with caution.

1.2.3 Ancillary Data

The CoreMetadata.0 and StructMetadata.0 HDF-EOS global attributes are stored in HDFEOS INFORMATION data group.

1.3 File Naming Convention

Example

AMSR_E_L3_SeaIce25km_V16_20080207.he5

Naming Convention

AMSR_E_L3_SeaIce25km_[X][##]_[YYYYMMDD].[EXT]

The following tables describe the variables in the file naming convention:

Table 2. File Name Variables and Descriptions

Variable	Description
X	Product maturity code: P, B, T, or V (See Table 3.)
##	File iteration number
YYYYMMDD	Four digit year, two digit month, two digit day
EXT	One of: • he5 (HDF-EOS5) • qa (quality assurance information) • ph (product history) • xml (granule-level science metadata)

Table 3. Product Maturity Codes

Variables	Description
P	Preliminary - refers to non-standard, near-real-time data available from NSIDC. These data are only available for a limited time until the corresponding standard product is delivered to NSIDC.
B	Beta - indicates a developing algorithm with updates anticipated.
T	Transitional - period between beta and validated where the product is past the beta stage, but not quite ready for validation. This is where the algorithm matures and stabilizes.
V	Validated - products are upgraded to Validated once the algorithm is verified by the algorithm team and validated by the validation teams. Validated products have an associated validation stage. Refer to Table 4 for a description of the stages.

Table 4. Validation Stages

Validation Stage	Description
Stage 1	Product accuracy is estimated using a small number of independent measurements obtained from selected locations, time periods, and ground-truth/field program efforts.
Stage 2	Product accuracy is assessed over a widely distributed set of locations and time periods via several ground-truth and validation efforts.
Stage 3	Product accuracy is assessed, and the uncertainties in the product are well-established via independent measurements made in a systematic and statistically robust way that represents global conditions.

1.4 Spatial Information

1.4.1 Coverage

North Polar Grid

N: 90.0° S: 30.98° E: 180.0° W: -180.0°

South Polar Grid

N: -39.23° S: -90.0° E: 180.0° W: -180.0°

The coverages specified above are shown in the following figures:

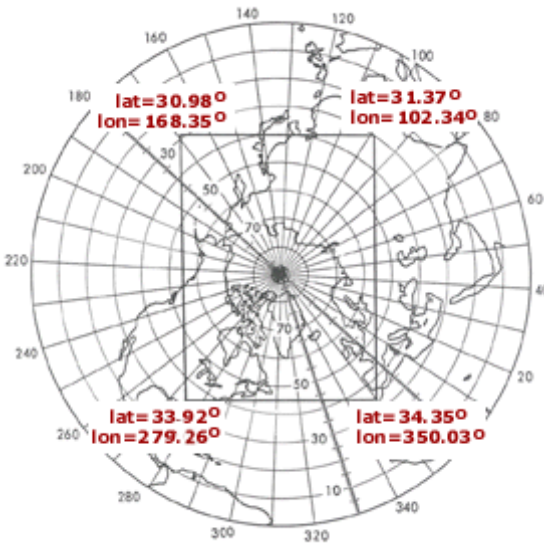

Figure 1. Northern Hemisphere Coverage

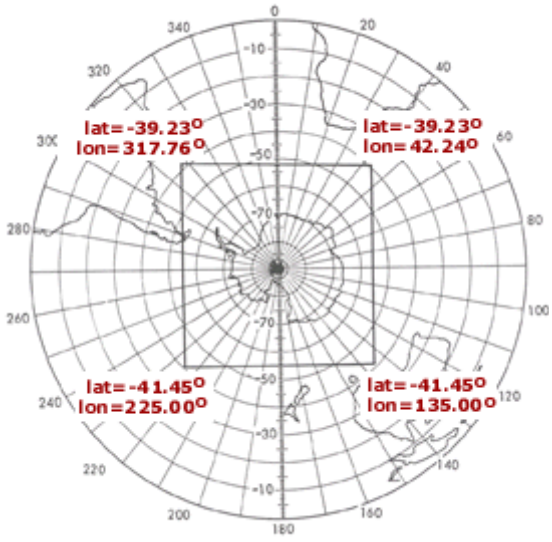

Figure 2. Southern Hemisphere Coverage

1.4.2 Resolution

25 km

1.4.3 Geolocation

The NSIDC polar stereographic grids specify a projection plane tangent to Earth at 70° latitude such that the projection is true at 70° rather than at the poles. This latitude was chosen so that little or no distortion would occur in the marginal ice zone.

The polar stereographic formula for converting between latitude–longitude and X–Y grid coordinates is taken from Snyder (1982). The projection assumes a Hughes ellipsoid with a radius of 6378.273 km (3443.992 nm) and an eccentricity of e = 0.081816153, or e^2 = 0.006693883. Note that this value of e^2 is stored to four significant digits (0.006694) in the HDF-EOS5 structural metadata (“HDFEOS INFORMATION/StructMetadata.0”).

The following tables provide information about geolocating this data set:

Table 5. Geolocation Details

Projected coordinate system	NSIDC Sea Ice Polar Stereographic North	NSIDC Sea Ice Polar Stereographic South
Geographic coordinate system	Unspecified datum based upon the Hughes 1980 ellipsoid	Unspecified datum based upon the Hughes 1980 ellipsoid
Longitude of true origin	-45	0
Latitude of true origin	70°	-70°

Projected coordinate system	NSIDC Sea Ice Polar Stereographic North	NSIDC Sea Ice Polar Stereographic South
Scale factor at longitude of true origin	1	1
Datum	Unspecified, based on Hughes 1980 ellipsoid	Unspecified, based on Hughes 1980 ellipsoid
Ellipsoid/spheroid	Hughes 1980	Hughes 1980
Units	meter	meter
False easting	0	0
False northing	0	0
EPSG code	3411	3412
PROJ4 string	+proj=stere +lat_0=90 +lat_ts=70 +lon_0=-45 +k=1 +x_0=0 +y_0=0 +a=6378273 +b=6356889.449 +units=m +no_defs	+proj=stere +lat_0=-90 +lat_ts=-70 +lon_0=0 +k=1 +x_0=0 +y_0=0 +a=6378273 +b=6356889.449 +units=m +no_defs
Reference	https://epsg.org/crs_3411/NSIDC-Sea-Ice-Polar-Stereographic-North.html	https://epsg.org/crs_3412/NSIDC-Sea-Ice-Polar-Stereographic-South.html

Table 6. Grid Details

Hemisphere	North Polar	South Polar
Grid cell size (km)	25 × 25	25 × 25
Grid size (rows × columns)	448 × 304	332 × 316
Geolocated lower left point in grid (km)	(-3850, -5350)	(-3950, -3950)
Nominal gridded resolution	25 km	25 km
Grid rotation	0	0
ulxmap: x-axis coord, center of upper left pixel (XLLCORNER) (km)	-3,838.5	-3,938.5
ulymap: y-axis coord, center of upper left pixel (YLLCORNER) (km)	5,838.5	4,338.5

For additional details about this projection, grid dimensions, and grid coordinates, see "A Guide to NSIDC's Polar Stereographic Projection."

1.5 Temporal Information

1.5.1 Coverage

01 June 2002 to 4 October 2011

1.5.2 Resolution

Daily

2 DATA ACQUISITION AND PROCESSING

2.1 Background

The NT2 sea ice concentration algorithm represents the most recent version of an approach that began in the 1970s with the “Bootstrap” algorithm. These algorithms—from the original Bootstrap algorithm, the Basic Bootstrap Algorithm (BBA), and the AMSR Bootstrap Algorithm (ABA), through the NASA Team algorithms, NT and NT2—all take advantage of the relatively high contrast in emissivity between open water and sea ice, highlighted by combining different pairs of channel data. Both the Bootstrap and NASA Team algorithms also employ filters to identify and remove spurious sea ice concentration estimates resulting from severe weather.

While the Bootstrap algorithms calculate ice concentrations by interpolating between data clusters in scatterplots of the 19V, 37V, and 37H channels, the NT algorithms compare polarization ratios (PRs) and spectral gradient ratios (GRs). For example, the original NT algorithm used primarily PR(19) and GR(37V19V), computed from the 19V, 19H, and 37V channels as follows:

$$PR(19) = \frac{T_b(19V) - T_b(19H)}{T_b(19V) + T_b(19H)}$$

$$GR(37V19V) = \frac{T_b(37V) - T_b(19V)}{T_b(37V) + T_b(19V)}$$

Similar to the Bootstrap approach, scatterplots of PRs vs GRs tend to cluster around different surface types, such as open ocean, 100% ice coverage, and in the Northern Hemisphere regions of first-year ice and multiyear ice (this distinction is unclear in Antarctica). To determine ice concentrations, the NT2 algorithm utilizes nine constant coefficients, or “tie points,” each representing a combination of surface type and channel (i.e., 19H, 19V, and 37V).

The enhanced NT2 algorithm (Markus and Cavalieri 2000) additionally incorporates the AMSR-E 89 GHz channels—specifically, PR(89), GR(89V19V), and GR(89H19H)—to resolve ambiguities between pixels with true low ice concentration and pixels with significant surface/weather effects.

While the 89 GHz channels have the added benefit of being relatively insensitive to inhomogeneities in ice surface layer characteristics (e.g., surface temperature variations), they exhibit a higher sensitivity to atmospheric effects. As such, the NT2 also implements a full atmospheric radiative transfer model plus two weather filters, to eliminate the effects of severe weather.

More detailed information is available from the following sources:

- Descriptions of and differences between the NASA Team and Bootstrap algorithms
- AMSR-E Algorithm Theoretical Basis Document: Sea Ice Products [Supplement 2012]
- AMSR-E Algorithm Theoretical Basis Document: Sea Ice Products [Supplement 2007]

2.2 Acquisition

This data set is derived from T_bs in the AMSR-E/Aqua L2A Global Swath Spatially-Resampled Brightness Temperatures (AE_L2A), Version 4 product.

2.3 Processing

The following sections summarize how the sea ice concentration and snow depth on sea ice calculations are implemented by the NT2 algorithm. For complete details, see “Section 2.2 | Implementation” in “AMSR-E Algorithm Theoretical Basis Document: Sea Ice Products [Supplement 2012]” (AMSR-E Sea Ice Products ATBD, 2012).

2.3.1 Sea Ice Concentration

In contrast to algorithms which compute sea ice concentrations from daily, averaged swath T_bs, the NT2 computes sea ice concentrations from individual swath T_bs, and then averages the concentrations to produce daily maps. This approach is critical for the NT2 because the atmospheric influence on T_bs is nonlinear and using averaged T_bs as input would dilute the atmospheric signal.

To determine sea ice concentration, the algorithm first computes T_bs for each AMSR-E frequency/polarization channel corresponding to each sea ice concentration-weather combination. The response of T_bs to different weather conditions is determined by a forward atmospheric radiative transfer model (Kummerow 1993), that utilizes input data based on Eppler et al. (1992)

and includes atmospheric profiles encompassing a range of cloud properties and average atmospheric temperature and humidity profiles for summer and winter conditions.

The algorithm then uses the weather-corrected T_bs to calculate PR and GR ratios and construct look-up tables. These same PR and GR ratios are then computed for the AMSR-E measured T_bs and compared with each of the ratios in the look-up tables to determine observed sea ice concentrations.

This procedure is detailed in “Section 2.2.1 | Calculation of ice concentrations” in the AMSR-E Sea Ice Products ATBD, 2012.

2.3.1.1 Land Spillover Correction

Although a land mask is applied to construct the final sea ice concentration maps, land spillover still leads to erroneous ice concentrations along coastlines adjacent to open water. To correct these errors, a five-step, land spillover correction scheme is applied to identify and delete all clearly erroneous ice concentrations. See “Section 2.2.2 | Land Spillover Correction” of the AMSR-E Sea Ice Products ATBD, 2012 for a complete description.

2.3.1.2 Weather Filters

Although the NT2 algorithm includes a forward atmospheric radiative transfer to provide weather-corrected sea ice concentrations, severe weather can still result in spurious concentrations over open ocean. As such, the algorithm implements two weather filters based on the spectral gradient ratios GR(37V19V) and GR(22V19V), with threshold values similar to those used by the NT algorithm. These filters are discussed in detail in “Section 2.2.3 | Reduction of Atmospheric Effects” of the AMSR-E Sea Ice Products ATBD, 2012.

2.3.2 Sea Ice Concentration Difference

This product also tracks the difference in estimated sea ice concentration between the AMSR-E Bootstrap Algorithm (ABA) and the NT2. This difference is calculated as ABA - NT2.

For details about the theory behind the ABA and its algorithmic implementation, the “AMSR-E Bootstrap Sea Ice Algorithm” ATBD is appended to the AMSR-E Sea Ice Products ATBD, 2012 (starting on page 14).

2.4 Quality Assessment

Each HDF-EOS file contains core metadata with Quality Assessment (QA) metadata flags that are set by the Science Investigator-led Processing System (SIPS) before delivery to NSIDC (this metadata is also available as a separate XML file).

2.4.1 Automatic QA

Automatic Weather filters are employed for the Level-3 sea ice products to eliminate spurious sea ice concentrations over open ocean resulting from varying atmospheric emission. The weather filters are based on threshold values for the spectral gradient radio and thresholds derived from brightness temperature differences. Sea ice products are checked to see if ice concentration values fall within reasonable limits. Diagnostics are based in part on satellite sea ice climatology developed since the Scanning Multichannel Microwave Radiometer (SMMR) era in 1978.

2.4.2 Science QA

AMSR-E Level-2A data are subject to science QA in the SIPS environment prior to being processed to higher-level products. Science QA checks for and computes the percentages of missing and out-of-range values for each variable, and If <50% of the data in a file are good, the file's science QA flag is marked suspect. Science QA also involves reviewing the operational QA files and performing the following additional automated QA procedures (Conway 2002):

- Historical data comparisons
- Detection of errors in geolocation
- Verification of calibration data
- Trends in calibration data
- Detection of large scatter among data points that should be consistent

Once a product passes QA, it is ready to be used for higher-level processing, active science QA, archive, and distribution. Individual files that fail QA are reprocessed before being sent to NSIDC. Files that fail QA are not delivered to NSIDC.

For more information, see the AMSR-E/Aqua Data Quality and Data Uncertainty document. In addition, users can access AMSR-E Validation Data that contain details about the accuracy and precision checks conducted on AMSR-E observations.

2.5 Error Sources

As a result of the spatial averaging when the Level 2A input data are produced, errors in neighboring observations within any single channel will be somewhat correlated (Errors between

channels are not correlated in any case). Thus, while the Level 2A data set are well suited for applications that require combining multiple channels of observations, users should be aware that errors in observations within a single channel may not be independent (Ashcroft and Wentz, 2000).

Users should also be aware that the ASC and DSC T_b averages are not computed as the average of all T_b observations, but as the average of the ASC and descending DSC averages. This can bias the daily value if, as shown by the following equation, the ASC and DSC averages on a given day were computed from different numbers of observations (i.e., n ≠ m):

$$DAY = \frac{\frac{ASC_1 + ASC_2 + \ldots ASC_n}{n} + \frac{DSC_1 + DSC_2 + \ldots DSC_m}{m}}{2}$$

Finally, although a land mask is applied to the ice concentration maps, land spillover still leads to erroneous ice concentrations along the coastlines adjacent to open water. A land spillover correction scheme is applied on the maps to help mitigate land spillover errors.

2.6 Instrumentation

Refer to the AMSR-E Instrument Description document.

3 VERSION HISTORY

See AMSR-E Version History for a summary of changes since the start of mission.

4 SOFTWARE AND TOOLS

4.1 Geolocation

Arrays of latitudes and longitudes at grid cell centers of the 25 km north and south polar stereographic grids are available in NetCDF format in the Polar Stereographic Ancillary Grid Information data set. The previous version of these grids (in binary format[2]) can be obtained via an FTP client from:

ftp://sidads.colorado.edu/pub/DATASETS/brightness-temperatures/polar-stereo/tools/geo-coord/grid/

[2]Latitudes/longitudes are stored as long word integers (4 byte) scaled by 100,000. Each (i,j) array location contains the latitude or longitude value at the center of the corresponding data grid cell.

In addition, NSIDC has a Fortran executable (locate.for) that allows a user to enter an (i,j) grid coordinate pair and obtain the corresponding latitude and longitude (and vice versa). locate.for, its required subroutines (mapll.for and mapxy.for), plus documentation are available from NSIDC's GitHub repository.

For more information, see "Does NSIDC have tools to extract and geolocate polar stereographic data? | Geocoordinate tools."

4.2 Land Masks

NSIDC provides masks and overlays that can be used, for example, to conceal unwanted northern and southern hemisphere land regions or contaminated coastal ocean pixels incorrectly assigned sea ice concentrations. To determine which masks are available for this data set, see "Does NSIDC have tools to extract and geolocate polar stereographic data? | Land Masks."

5 REFERENCES AND RELATED PUBLICATIONS

Ashcroft, P. and F. J. Wentz. 2000. *Algorithm Theoretical Basis Document (ATBD): AMSR Level 2A Algorithm*. Revised November 3. Landover, Maryland USA: Goddard Space Flight Center. (PDF)

Cavalieri, D. and J. Comiso. 2000. *Algorithm Theoretical Basis Document for the AMSR-E Sea Ice Algorithm*, Revised December 1. Landover, Maryland USA: Goddard Space Flight Center. (PDF)

Cavalieri, D. J., K. M. St. Germain, and C. T. Swift. 1995. Reduction of Weather Effects in the Calculation of Sea Ice Concentration with the DMSP SSM/I. *Journal of Glaciology* 41(139): 455-464.

Cavalieri, D. J., P. Gloersen, and W. J. Campbell. 1984. Determination of Sea Ice Parameters with the NIMBUS-7 SMMR. *Journal of Geophysical Research* 89(D4): 5355-5369.

Comiso, J., D. Cavalieri, and T. Markus. 2003. Sea Ice Concentration, Ice Temperature, and Snow Depth using AMSR-E data. *IEEE Transactions on Geoscience and Remote Sensing* 41(2): 243-252.

Comiso, J. and K. Steffen. 2001. Studies of Antarctic Sea Ice Concentrations from Satellite Data and Their Applications. *Journal of Geophysical Research* 106(C12): 31,361-31,385.

Comiso, J. C., D. J. Cavalieri, C. L. Parkinson, and P. Gloersen. 1997. Passive Microwave Algorithms for Sea Ice Concentration - A Comparison of Two Techniques. *Remote Sensing of the Environment* 60: 357-384.

Comiso, J. C. 1995. *SSM/I Ice Concentrations Using the Bootstrap Algorithm*. NASA RP 1380.

Conway, D. 2002. *Advanced Microwave Scanning Radiometer - EOS Quality Assurance Plan*. Huntsville, AL: Global Hydrology and Climate Center.

Eppler, D. T. and 14 others. 1992. Passive Microwave Signatures of Sea Ice in Microwave Remote Sensing of Ice. *Geophysical Monograph Series* 68: 47-71.

Fraser R. S., N. E.Gaut, E. C. Reifenstein, and H. Sievering. 1975. Interaction Mechanisms Within the Atmosphere Including the Manual of Remote Sensing. *American Society of Photogrammetry* 181-233. Falls Church, VA.

Gloersen P. and D. J. Cavalieri. 1986. Reduction of Weather Effects in the Calculation of Sea Ice Concentration from Microwave Radiances. *Journal of Geophysical Research* 91(C3): 3913-3919.

Gloersen P, W. J. Cambell, D. J. Cavalieri, J. C. Comiso, C. L. Parkinson, and H. J. Zwally. 1992. *Arctic and Antarctic Sea Ice, 1978-1987: Satellite Passive Microwave Observations and Analysis*. Washington, D.C.: National Aeronautics and Space Administration, Special Publication 511.

Kummerow, C. 1993. On the Accuracy of the Eddington Approximation for Radiative Transfer in the Microwave Frequencies. *Journal of Geophysical Research* 98: 2757-2765.

Lubin, D., C. Garrity, R. O. Ramseier, and R. H. Whritner. 1997. Total Sea Ice Concentration Retrieval from the SSM/I 85.5 GHz Channels During the Arctic Summer, *Remote Sensing of Environment* 62: 63-76.

Markus, Thorsten and Donald J. Cavalieri. 2008. [Supplement] AMSR-E Algorithm Theoretical Basis Document: Sea Ice Products. Greenbelt, Maryland USA: Goddard Space Flight Center.

Markus, Thorsten and Donald J. Cavalieri. 1998. Snow Depth Distribution over Sea Ice in the Southern Ocean from Satellite Passive Microwave Data. IN: *Antarctic Sea Ice: Physical Processes, Interactions, and Variability*. *Antarctic Research Series* 74:19-39. Washington, DC, USA: American Geophysical Union.

Markus, Thorsten and Donald J. Cavalieri. 2000. An Enhancement of the NASA Team Sea Ice Algorithm. *IEEE Transactions on Geoscience and Remote Sensing* 38: 1387-1398.

Markus, T., D. Cavalieri, and A. Ivanoff. 2011. Algorithm Theoretical Basis Document for the AMSR-E Sea Ice Algorithm, Revised December 2011. Landover, Maryland USA: Goddard Space Flight Center. (PDF file, 528 KB)

Matzler, C., R. O. Ramseier, and E. Svendsen. 1984. Polarization Effects in Sea-ice Signatures. *IEEE Journal of Oceanic Engineering* 9: 333-338.

Pearson, F. 1990. *Map projections: Theory and Applications*. Boca Raton, FL: CRC Press.

Snyder, J.P. 1987. *Map projections - a Working Manual*. U.S. Geological Survey Professional Paper 1395. U.S. Government Printing Office. Washington, D.C.

Snyder, J. P. 1982. *Map Projections Used by the U.S. Geological Survey.* U.S. Geological Survey Bulletin 1532.

6 RELATED DATA SETS

- Sea Ice Data at NSIDC
- Sea Ice Trends and Climatologies from SMMR and SSM/I-SSMIS

7 CONTACTS AND ACKNOWLEDGMENTS

Thorsten Markus, **Josefino C. Comiso, and Linette Boisvert**
NASA Goddard Space Flight Center
Greenbelt, MD

Walt N. Meier
National Snow & Ice Data Center
Boulder, CO

8 DOCUMENT INFORMATION

8.1 Publication Date

July 2025

8.2 Date Last Updated

July 2025